Title
Cross-Sectional Transmission Electron Microscopy of X-Ray Thin Film Multilayer Structures

Journal
Journal of electron microscopy technique, 19

Authors
Nguyen, T.D.
Gronsky, R.
Kortright, J.B.

Publication Date
1991-08-01

LBL-29841
Preprint

Lawrence Berkeley Laboratory
UNIVERSITY OF CALIFORNIA

Accelerator & Fusion
Research Division

Center for X-Ray Optics

Submitted to Journal of Electron Microscopy Technique

Cross-Sectional Transmission Electron Microscopy of X-Ray Thin Film Multilayer Structures

T.D. Nguyen, R. Gronsky, and J.B.Kortright

August 1991

Prepared for the U.S. Department of Energy under Contract Number DE-AC03-76SF00098

DISCLAIMER

LBL -29841

CROSS-SECTIONAL TRANSMISSION ELECTRON MICROSCOPY OF X-RAY THIN FILM MULTILAYER STRUCTURES

Tai D. NGUYEN,[1,2] Ronald GRONSKY,[2] and Jeffrey B. KORTRIGHT[1]

[1]Center for X-Ray Optics,
[2]National Center for Electron Microscopy,
Lawrence Berkeley Laboratory,
University of California, Berkeley, CA. 94720

This work was supported by the director, Office of Energy Research, Office of Basic Sciences, Materials Sciences Division, of the U.S. Department of Energy under Contract No. DE-AC03-76SF00098 and by the Air Force Office of Scientific Research, of the U.S. Department of Defense under Contract No. F49620-87-K-0001.

CROSS-SECTIONAL TRANSMISSION ELECTRON MICROSCOPY OF X-RAY THIN FILM MULTILAYER STRUCTURES

ABSTRACT

A simple method for preparing cross-sectional Transmission Electron Microscopy specimens and discussions of possible artifacts from specimen preparation and observation of x-ray multilayer thin film structures are presented. The intent of the paper is to provide the beginners in the field a step-by-step procedure to prepare the samples. The specimen preparation method employs mechanical grinding and polishing to approximately 20 μm, followed by ion milling, without dimpling. Artifacts such as preferential ion milling and crystallization under the electron beam, as well as effects of Fresnel fringes at interfaces, are important factors in interpretation of the images. Care in identifying them is required to avoid erroneous results in studies of morphology and microstructures within the layers and at their interfaces. Example High-Resolution TEM results of cross-sectional W/C, Ru/C, and Mo/Si, multilayers are presented.

INTRODUCTION

Multilayer structures of nanometer periods have been widely used in x-ray optical applications as dispersive elements for radiation of ultraviolet to x-ray wavelengths (Marshall, 1985). These structures typically consist of alternating layers of high and low atomic number materials, with the bilayer periods governed by the operating wavelengths and angles according to Bragg's equation. The performance of these multilayers may depend on the microstructures and homogeneity of the layers and their interfaces. These

devices must have smooth layers, atomically sharp interfaces, and precise period thicknesses for optimum performance. The two materials comprising the layers must also be resistant to interdiffusion and chemical reaction. Characterization of the internal microstructures is therefore of great importance since it aids in an understanding of the multilayer quality and performance.

Various techniques have been employed to characterize such x-ray optical multilayer structures. These include x-ray reflectance measurements of the specular radiation reflected by the composition modulation, scattering from the interatomic structures (Kortright, 1988; Takagi, 1985), and EXAFS (Lamble, 1988). X-ray characterization methods characteristically provide structural information averaged over a relatively large area, and are insensitive to local variations and reactions inside the individual layers. Local structural information is obtained from the cross-sectional transmission electron microscopy technique, and thus yields complementary data to that obtained from the x-ray techniques. Cross-sectional TEM has the advantage that it allows observation of all the layers and their interfaces at the same time. In addition, HRTEM of cross-sectional specimens can provide valuable microstructural and morphological information about the layers and associated interfacial phenomenon at the atomic scale. The difficulty of cross-sectional TEM, however, is the preparation of the specimens to render the multilayers transparent to the electron beam, and the interpretation of the resultant TEM images.

Cross-sectional TEM specimens of x-ray multilayer thin film structures, similar to those of electronic or dielectric materials, are generally prepared by mechanical thinning and subsequent ion milling, as first described by Abrahams and Buiocchi (1974), and further developed by various groups (Sheng and Marcus, 1980; Baxter and Stobbs, 1985; Garulli et al., 1985; Holloway and Sinclair, 1987). Special techniques such as mechanical dimpling prior to ion milling (Bravman and Sinclair, 1984; Vanhellemont et al., 1983; 1988; Shinde and De Jonghe, 1986), the appplication of beam shields to the specimen stage (Helmersson and Sundgren, 1986; Chang et al., 1988), and the use of masks over the

specimens (Santella et al., 1988) to prevent subsequent preferential ion beam thinning, have been reported. An alternative preparation procedure that omits the ion milling step by using a special tool for direct mechanical thinning to less than 1 μm thick, has also been developed recently (Benedict et al., 1990). In addition to the method of mechanical thinning and ion milling, cross-sectional TEM samples of x-ray multilayers have also been prepared by microcleavage (Lepetre et al., 1985) and ultramicrotomy (Swab and Klinger, 1988).

Although many cross-sectional TEM results on different x-ray optical multilayer systems have been reported (Lepetre et al., 1986; Petford-Long et al., 1987; Gronsky and Punglia, 1987; Holloway et al., 1988), only a few have discussed the difficulty of interpretation of the results (Baxter and Stobbs, 1985), the possibility of artifacts induced by sample preparation and TEM observation (Ruterana, 1989), and specimen heating effects during ion beam milling (Kim and Carpenter, 1987; Bahnck and Hull, 1990). In this paper, we present a simple step-by-step method for preparing cross-sectional TEM specimens of the x-ray multilayer thin film structures, discuss the interpretation of the results, and describe possible artifacts from both specimen preparation and electron irradiation during TEM imaging.

MATERIALS AND METHODS

1. Multilayer Sputtering

For this study, thin films were deposited onto 3 inch-diameter, [001] or [111] semiconductor-grade silicon wafer substrates. Bilayers of alternating high and low atomic number materials were produced by magnetron sputtering onto an amorphous carbon buffer layer that was intended to attenuate the atomic-scale roughness of the Si substrates. The Si

substrate materials were best viewed along the <110> direction, which is perpendicular to the flat edge of the Si wafer. This ensured that the multilayers were imaged edge-on since the substrate miscut was directed along [112], and that the {111} planes (d_{111} = 0.3135 nm) were resolvable under phase contrast imaging conditions so that they could be used for an internal magnification calibration.

2. Sectioning

The complete specimen preparation procedure is illustrated in figure 1. First, two slabs of the silicon substrate sample, 10 mm long by 3 mm wide, are cut, with the longer side of the slabs parallel to the flat edge of the Si wafer, using a diamond-scribe (figure 1a). The orientation of the cut will yield a <110> direction parallel to the electron beam when viewed in the microscope, and the dimensions of these slabs are just enough for two samples to be mounted on 3mm-diameter TEM grids after mechanical thinning. If the samples are scarce or difficult to obtain, a thinner sample can be used, as described in the method of Garulli et al. (1985). The two slabs are glued together using epoxy, with the deposited films facing each other as shown in figure 1b. This provides mutual protection for the multilayer thin films against breakage and fracture during thinning. Several epoxies have been reported to provide good adhesion, such as BUEHLER Epoxide Resin and Hardener (Garulli et al., 1985), and the widely used M-Bond 610 adhesive (Bravman and Sinclair, 1984). However, the BUEHLER Epoxide has to be stored over night for the resin to be completely polymerized, and the M-Bond 610 must be thermally set under pressure for two hours. In this experiment, we use Devcon 2-ton epoxy, which is cured by thermoseting at a temperature of about 90°C for 30 minutes, or at room temperature over night. This epoxy does not require the use of a vise to press the sample slabs together during curing; however, a vise can be used if there is concern for the thickness of the epoxy layer between the samples.

3. Mechanical Thinning

The glued sandwich is mechanically thinned using sandpaper on a rotating grinding wheel, and polished using alumina powder on polishing cloths. To start, the sandwiched sample is mounted on a 1 inch-diameter 5/8 inch-thick piece of Pyrex glass, using Crystal Bond 509 wax by Aremco Products, Inc. Although the glass can be made of any size, it is found that this size is the most stable to hold and handle during thinning. The glass piece, with a small volume of the Crystal Bond, is placed on top of a hot plate set at about 300°C. Only a very small volume of the Crystal Bond is required, just enough to cover the entire bottom of the sandwich-like sample, to hold it to the glass. The wax usually melts within about 5 minutes. The sample is then carefully mounted on top of the glass, ensuring that the film surfaces are perpendicular to the surface of the glass, so that the sample is mechanically thinned perpendicular to a <110> direction.

The sample is first thinned using 600-grit paper (20 μm silicon carbide particles) on a rotating grinding wheel, as illustrated in figure 1c. During grinding, ample water is made to run over the sandpaper so that the wax does not heat up and melt. The top surface of the sandwich-like sample is kept as parallel to the glass surface as possible. Throughout all the thinning and polishing steps, the motion of the sample relative to the paper is controlled to keep the movement parallel to the films or the interfaces, and minimize mechanical stresses.

The sample is ground on one side parallel to the glass surface, but leaving it thick at this point for easier handling, then polished to a specular finish. After mechanical thinning, a pre-polishing step might be added to expedite the polishing procedure. In this step, the sample is polished by moving back and forth on 2400-grit paper (5 μm), under distilled water to keep it cool. The polishing motion is again parallel to the films or the interfaces. This step does not thin the sample as much as it smoothes the surface before subsequent polishing. At this point, the surface should have a specular finish. The sample is then polished using 1 μm alumina, and followed by 0.05 μm alumina, on a polishing cloth and

rotating wheel (figure 1d).

After polishing the first side, the glass base holding the sample is again placed on the hot plate. When the wax between the sample and the glass is partially melted, the sample is turned over, so that the polished side is facing toward the glass piece. A pair of tweezers is used to press the sample down firmly onto the glass base while the wax is cooling, so that the wax layer between the sample and the glass base is as thin as possible, to increase the accuracy of the thickness measurement of the thinned sample, as explained below.

Following the same steps as before, the newly exposed side is thinned and polished, using 600-grit paper, 2400-grit paper, 1 μm alumina, and 0.05 μm alumina. However, the sample is now thinned to about 20 μm before being polished. Care must be taken so that the sample is not broken or ground away since the sample becomes more fragile the more it is thinned. The use of a glass support for mechanical thinning enables the observation of the sample condition and its thickness during the thinning operation. Polishing both sides of the cross-section sample will ensure an even milling rate at the center of the sample from both sides. Although larger alumina powders could be used in the final polishing step, it is our experience that the finer the surface polish the better the ion milling operation.

During thinning, the thickness of the sample is measured frequently, to estimate the thinning rate. The thickness of the cross-section sample on the glass piece is determined by using a micrometer, or a depth-probing optical microscope equipped with vernier scale focussing knob. The sample thickness is the difference between the thickness of the glass piece with the sample, and the thickness of the glass piece alone, measured by the micrometer. An optical depth-probing microscope, if available, is used to measure the specimen thickness more accurately when the specimen is ultra-thin. The difference between the two readings, taken when the microscope is focused on the specimen surface, and when focused on the glass surface, gives the sample thickness. The measured thickness is slightly greater than the actual thickness, due to the thin layer of wax between the glass

and the sample. The accuracy of these techniques are normally satisfactory for this experiment, although a major source of error could be the uneven surface of the glass base. In general, the specimen is thinned until the edges start to regress. This is a sign that the second side is ready for polishing.

Pre-polishing and polishing steps are carried out as for the first side, but with even more care now that the specimen is extremely thin and delicate. After polishing, the sample is ready to be mounted on TEM grids for ion milling.

If a dimpling machine is available, the thinning process could follow a slightly different method, suggested by Bravman and Sinclair (1984). Many 3 mm x 7 mm slabs of samples on Si substrates are cemented together, to make up a 3 mm-square by 7 mm long piece, with the films of each slab facing toward the center. The sample is thinned to about 200 μm, then cut into a 3 mm-diameter disc by using a slurry drill or an ultrasonic impact grinder, and thinned again to about 100 μm. Before ion milling, the sample is dimpled by a small "grinding" wheel, which contacts the rotating 3 mm-diameter disc sample on one side, thinning the sample down in a bowl-shaped geometry. This yields a central depression of approximately 20 μm thick with an outer perimeter of thicker, more sturdy material. The use of the dimpler is highly recommended, although there are risks associated with slurry drilling or ultrasonic cutting.

4. Ion Milling

The 20 μm-thick sample is next mounted on a TEM grid to be ion milled. The grids are cemented onto the sample to create a support for the sample before removing it from the glass base, allowing easy control and reducing the chance of breakage during handling. Two small drops of the epoxy are placed on the sample at about the length of a grid apart, using a pointed wooden stick. The 0.5 mm-width oval-slot TEM grids are then placed on top of the thinned sample, such that the film surfaces or interfaces are parallel to the longer

side of the slot, and the sample covers the entire slot, as shown in figure 1e. Only a small drop of epoxy is required at each application point; excess epoxy will also bond the sample or the grid to the glass base, making it difficult to retrieve the sample later. The epoxy is then cured at 90°C for 30 minutes, or over night at room temperature.

After curing, the specimens are separated by carefully using a pair of tweezers to break off excess sample around the 3 mm-diameter grids. Removal of the specimens from the glass base can be done by submerging the glass base with the specimens attached in warm acetone until the wax is completely dissolved, or by placing the glass base on a hot plate to soften the wax, sliding the sample grids in the direction parallel to the films until they overhang the glass base, removing them with tweezers, and soaking in warm acetone for about 15 minutes to remove the remaining wax.

The sample in this study was ion-milled in a cold stage Gatan "Dual Ion Mill" Model 600, with argon ion guns bombarding on both sides of the specimen, schematically shown in figure 1f. The argon ions were first accelerated with a voltage of 5 kV, drawing a specimen current of 0.5 milliamps, at a specimen tilt angle of 13°, under 10^{-4} torr pressure during milling. By employing a laser auto-terminator, an accessary attachment to the ion milling machine available from Gatan, the specimen is left in the ion milling machine until the ion source is automatically switched off when perforation is achieved. This usually takes about 4 to 6 hours, depending on the thickness of the sample and the aperture of the ion guns. To facilitate an auto-terminator, the sample has to cover the grid slot completely, which is why the small-width oval-slot TEM grids are used. Since the ion milling rate of the epoxy is generally faster than that of the Si substrate, the ion beam bombardment usually makes a hole in the epoxy first. Once perforation is achieved, the sample is ion milled for about an hour more, with the tilt angle reduced to 11°, in order for the sample to have a shallower thickness gradient for TEM observation. Smaller tilt angles might cause re-sputtering of some unwanted particles onto the sample from the inner edges of the grid, and should be avoided. After the ions have created a hole along the epoxy about 1 mm long,

as illustrated in figure 1g, with the areas for possible TEM observation arrowed, it is exposed again to an ion beam of 3.0 kV potential, 0.3 milli-amp current, for another 15 to 30 minutes. This last step does not thin the sample any further but is used to remove any "overlayers" of damaged, amorphous material on the specimen which builds up as a result of ion bombardment. The sample is now ready to be studied in a microscope. Figure 1h shows a cross-sectional TEM image of a multilayer prepared by this method.

Samples made up of 4 or 6 slabs, similar to that described by Bravman and Sinclair (1984), mounted on a 1 mm-width oval-slot grid, have been tried. The advantage of this configuration is that a lower ion milling angle (10°) can be used, without the danger of resputtering of grid material onto the specimen. It was found, however, that perforation and further ion beam thinning usually take place not at the epoxy between the center slabs, but at the epoxy layers between the center slabs and the outer ones, since after mechanical thinning, the sample is generally thinner closer to the edges than at the center.

5. Electron Microscopy

Transmission electron microscopy of the specimens was performed in a JEOL JEM 200CX equipped with ultrahigh resolution goniometer, operating at 200 kV. Image acquisition and observation under the electron beam were carried out quickly and carefully to ensure that minimum exposure to the beam was achieved, and no radiation damage occured. When a thin region was identified, the sample was tilted to a [110] Si pole while the beam was on the silicon substrate, not the multilayers. The beam was then defocused, and moved to the multilayer region. The multilayer was then focused and adjusted for astigmatism at as broad a defocused beam as possible, to reduce radiation exposure from the electron beam. A through-focus-series of images was then recorded. The use of a liquid nitrogen cold trap at the specimen stage also helped to minimize thermal build up at the sample, deterring any interfacial interdiffusion or interface motion, or crystallization of

the layers during ion beam energy acquisition (Kim and Carpenter, 1987).

6. Image Interpretation

Many artifacts can be induced during the ion milling step, or under the electron beam during observation. Milling at high voltage and current may lead to crystallizaion or recrystallization of the layers, and to the formation of an amorphous layer covering the ion-milled specimen. Both events could cause erroneous interpretation of the structures and phases present in the multilayers. The use of the cold stage ion mill at liquid nitrogen temperature helps to prevent recrystallization of the materials under the intense electron beam, and to minimize phase transformations within the constituents.

In this experiment, signs of crystallization from ion milling were rarely observed, and they were checked carefully for consistency with other areas of the same multilayer to guarantee that it is the true interpretation and not an artifact induced during specimen preparation.

a) Ion Milling Artifacts

Ion milling usually forms an amorphous overlayer on the specimen, which may cause an increase in the background noise level of the image and the diffraction pattern. The presence of this layer is seen as this band about 30Å wide at the edge of the observed areas; it appears at the edge of the 20 Å period W/C multilayer shown in figure 2. This layer is usually removed, or minimized, by employing the last step in the ion milling process where the sample is ion milled at low voltage and current for about 15 minutes, as described earlier. This step, acting as a cleaning step, effectively removes the overlayer without damaging or thinning the underlying sample any further.

Preferential ion milling is sometimes observed in the multilayer samples. In x-ray

multilayer structures with alternate layers of very different atomic number, such as W and C, ion milling could be quite difficult. The light and low density carbon has a significantly higher ion milling rate than the heavier and higher density W. This difference occasionally results in the preferential ion milling of the C layers, leaving the W layers exposed, as can be seen in figure 3, which shows the image of a 7 nm period W/C multilayer that has been annealed at 500°C for 4 hours in vacuum. As the carbon layers are removed, the remaining W layers often separate or collapse, locally altering the periodicity of the multilayer structures. This coalescence or separation of the W layers, and disappearance of the carbon layers, has also been observed by Ruterana et al. (1988), who cited long exposure under the electron beam as the cause. By contrast, the W-rich layers in figure 3 recrystallized as a result of prior external thermal annealing, and not from ion beam damage. This has been confirmed by consistent observation of many areas of the same multilayer sample, and of plan-view samples prepared without ion milling. (Nguyen et al., 1989; 1990a)

Another problem which may arise during ion milling is the re-deposition of material that has been removed by the ion beam when it strikes contiguous parts of the sample or its holder. The final cleaning step at the end of the specimen preparation process can also effectively remove these extraneous overlayers.

b) Artifacts from irradiation and interpretation

Careful and systematic observation of the images are required to avoid misinterpretation of the results. The images taken at an area of a multilayer were checked with other areas of the same multilayer to ensure that that area shows the representative structures of the multilayer. Figure 4, for example, shows the electron image of a 7 nm period W/C multilayer, in which the layers at the central part of the image appear to be different from the surrounding areas. These layers are not quite as uniform, their interfaces are not as sharp, and seem to indicate the presence of interdiffusion of the W

and C layers; these are not "representative" features of the surrounding microstructure. This phenomenon probably resulted from either excessive bombardment of the ions to that area in the ion milling process, or irradiation damage under the electron beam during image observation. These causes could result in differences in the structures of the layers and at the interfaces, and sometimes even induce more diffusion and/or recrystallization through the layers.

1. Layer Thickness Variations

The thickness gradient of the wedge-shaped ion milled sample and possible bending of the thin sample under the electron beam can result in apparent variations in relative thicknesses of the two layers in a multilayer period. The projection of the layers onto the image plane could show a broadening of the high atomic number layer thickness in the image. The multilayers were imaged at exact <110> Si which means that the layers were viewed edge-on. The multilayers can also be aligned edge-on with the electron beam using the diffraction spots arising from the bilayer periodicity in the low angle diffraction patterns (Holloway and Sinclair, 1987). By either alignment method, the apparent relative thickness variation, as shown in a multilayer in figure 5, still can be observed and is more severe in thicker region where the projection length is longer for the same angle of tilt. Rough interfaces between the layers further contribute to the increased apparent thickness of the high-Z layers in the projection at larger specimen thickness (Ruterana et al., 1989). The effect can yield qualitatively the thickness gradient of the ion milled sample, but does not give an accurate measurement of the layer thicknesses. The bilayer thickness of the multilayers as imaged is still conserved when measured at the thicker specimen regions; however, the composition of each layer is not properly represented in these regions. The individual layer width is determined more accurately at the thinner region of the specimen. A more precise determination of the locally averaged period of the multilayers is usually

measured from the selected area diffaction pattern of the multilayers, using the 111 silicon spots (d=3.14 Å) as calibration.

2. Interfacial structures

Because of the many problems associated with the understanding of these multilayers, the determination of their interfacial structure and morphology is crucial and, at the same time, tedious. Preferential thinning and the corresponding effect of a specimen thickness gradient, coupled with possible bending of the specimens in the thinner regions, may alter the structures of the interfaces imaged in the micrographs. Preferential milling and electron irradiation may also cause intermixing between the constituent layers, which yields extraneous structures at the interfaces. The removal of the carbon layers by preferential elemental milling destroys the interfaces between the W and C layers. It is also possible that there may be a local thickness gradient at the W/C interfaces, which appears as a density gradient in the images, although this is not confirmed. Regions of the sample that are wedge-shaped or misoriented appear to have variations in layer thickness, giving a false impression of the composition of the W and C layers, and the structure and thickness of the interfaces. The projected image of the misoriented layers also suggests a density gradient at the interfaces, giving an impression of the existence of finite interfacial layers, or interdiffusion of the two layers. In fact, the interfaces may be very sharp and uniform and still give this false impression.

Another difficulty in interpreting the structures and morphology of the layer interfaces from the electron micrographs arises from the presence of Fresnel fringes at the interfaces (Nguyen et al., 1990b; Shih and Stobbs, 1990). These fringes result from the electrons experiencing an abrupt change in the inner scattering potential between the high-Z and low-Z layers. The fringe visibility is more pronounced with increasing defocus away from minimum contrast, and shows opposite contrast at positive and negative defocus

values. This characteristic can be seen in figure 6, which shows contrast and spacing variations of Fresnel fringes with defocus values in a through-focus-series of a 9 nm period Mo/Si multilayer structure. Images taken at different defocus values hence can give different impressions of the sharpness and interdiffusion at the interfaces. Fresnel fringe effects, however, can provide an alternative technique for the characterization of interfaces in multilayer structures. Quantitative analysis (Shih and Stobbs, 1990) or computer simulation (Nguyen et al., 1990c), in fact, may yield useful information on the morphology or composition at these interfaces. The images presented were taken as close to the Scherzer defocus as possible for consistency.

RESULTS AND DISCUSSION

Figure 7 shows a typical HRTEM image of a W/C multilayer in cross-section. Features include the Si substrate, the C buffer layer, 50 bilayers of tungsten and carbon, the epoxy layer, and the top layers of the multilayer from the other sample slab used to make up the specimen sandwich. The epoxy layer is measured to be only about 80 nm thick. The thickness of each bilayer is approximately 7 nm, composed of 60% the W-rich layer, and 40% the C-rich layer. The field of view of the thin area under observation is more than 500 nm wide. At this magnification the layers appear to be smooth, and flat across the interfaces. Closer inspection of the layers and their interfaces is possible using the phase contrast imaging technique at higher magnification, as shown in figure 8. The lattice image of the (111) planes of the Si substrate are clearly visible, providing an internal calibration (d_{111} = 3.14 Å) for measurement of the image. The thickness of the carbon buffer layer is approximately 8 nm. The intended thicknesses of the C and the W layers were 4.2 nm and 2.9 nm, respectively. Measurement from the image, however, seemed to show a slightly thicker W and thinner C layers. This may be the thickness variation as a result of imaging

rough interfaces as discussed in an earlier section. Both the W-rich and C-rich layers seemed to show predominantly amorphous structure. Some evidence of micro-crystallinity can be observed in the W-rich layer at the thinnest area near the edge of the sample, although it could be an artifact from ion milling. Observation of crystallinity was confirmed further by examining the layers far from the edge of the sample, and the electron diffraction pattern, which did not indicate any obvious sign of crystallinity in this case. A detailed study of the as-deposited and annealed tungsten - carbon system was reported earlier by Nguyen et al. (1989).

Other systems under study are Ru/C and Mo/Si multilayers. Figure 9 shows a HRTEM image of a Ru/C multilayer, with its diffraction pattern shown in the inset. The layers in this specimen are quite linear and uniform, with some evidence of intermixing between the layers. Local interfacial roughness seen at the top layers probably results from extensions of the Ru crystalline planes or grain boundaries into the amorphous carbon layers (Nguyen, 1990). In those regions where the interfacial layers are typically only few angstrom thick, it is difficult to interpret the origin of the image contrast, which could either be from interdiffusion of the components, or of Fresnel fringe formation. The period of the multilayer is determined to be 4.3 nm. The carbon-rich layers are predominantly amorphous, while the Ru layers, which were intended to be less than 2 nm thick in each layer, clearly exhibit some crystalline phase throughout the layers. The diffraction pattern shows the [110] zone axis along which the Si substrate was imaged, the finely spaced diffraction spots arising from the periodicity of the multilayer, and the diffuse ring from the Ru crystals. The multilayer period determined from the diffraction spots is 4.27 nm, which agrees quite well with that obtained from the bright field image. It is also noted that the layers are inclined toward [112] at appproximately 4.5° from [111] of the substrate, consistent with typical miscut values.

High resolution electron micrographs of a 9 nm period Mo/Si multilayer are shown in figure 10. In this multilayer, a Mo layer was deposited first, without the deposition of a

carbon buffer layer. The effect of the buffer layer has not been studied extensively, however, Ruterana et al. (1989) showed that multilayers deposited over a rough substrate usually smooth themselves out after about ten layers even without a buffer layer. The thin layer between the Si substrate and the first Mo layer, as can be seen in figure 10a, is the native oxide layer built on the surface of the Si substrate, and has a typical thickness of about 1.5 nm. The layers at this low magnification seem both smooth and linear. Shown in figure 10b is an enlarged image of a region near the edge of the multilayer in figure 10a. At this magnification, the crystalline fringes in the Mo layers are clearly visible over a long lateral extent. The Si layers are amorphous, as confirmed by the electron diffraction pattern. The interfacial layers on the two sides of the Mo layers appear symmetrical, as also observed in a sputtered Mo/Si multilayer by Chang et al. (1989). The diffraction pattern in figure 10c shows the (110) ring of pure Mo, with a preferred orientation perpendicular to the multilayer surface.

CONCLUSIONS

A simple method for the preparation of x-ray multilayers in cross-sectional configuration for TEM has been described. Using this technique, a set of samples can be mechanically prepared in less than 3 hours, followed by 4 to 6 hours in the ion milling machine, with a high success rate. The technique can be applied to most thin film structures where cross-sectional analysis is needed. A summary of the steps for preparation of cross-sectional TEM specimen is as follows:

1) Cut materials into 10 mm x 3 mm slabs (figure 1a).

2) Form sandwich-like sample and mount on a glass support (figure 1b).

3) Mechanically thin and polish both sides of the sample to approximately 20 μm thick (figures 1c-d).

4) Mount the TEM grids on the sample (figure 1e).

5) Ion mill the sample (figure 1f).

Direct observation of the microstructures and phases present inside the layers, the morphology of the interfaces, and the uniformity of multilayer structures can be made with this cross-sectional TEM method. Many artifacts, however, can be induced during the ion milling step or the observation process, such as preferential ion milling and crystallization under the electron beam. Possible bending of the specimen under the beam and Fresnel fringe effects at interfaces can cause misinterpretation of the individual layer thickness and interfacial structures difficult. Recognition of these artifacts is essential in obtaining high quality images and avoiding their erroneous interpretation.

ACKNOWLEDGEMENT

The authors would like to thank John Turner of National Center for Electron Microscopy, Lawrence Berkeley Laboratory, for his assistance in preparing the photographs in the specimen preparation method section.

REFERENCES:

Abrahams, M.S., and Buiocchi, C.J. (1974) Cross-section specimens for transmission electron microscopy. J. Appl. Phys, 45:3315-3316.

Bahnck, D, and Hull, R. (1990) Experimental measurement of transmission electron microscope specimen temperature during ion milling. In: Workshop on specimen preparation for transmission electron microscopy of materials II. Anderson, R., ed. (Mat. Res. Soc. Proc.).

Baxter, C.S., and Stobbs, W.M. (1985) TEM methods for the characterisation of fine metal multilayers. Ultramicroscopy, 16:213-226.

Benedict, J.P., Anderson, R., and Klepeis, S.J. (1990) A procedure for cross sectioning materials for TEM analysis without ion milling. In: Proceedings of the Twelve International Congress for Electron Microcopy.

Bravman, J.C., and Sinclair, R. (1984) The preparation of cross-section specimens for transmission electron microscopy. J. Electron Microsc. Tech., 1:53-61.

Chang, C.-H., Stearns, M.B., and Smith, D.J. (1989) Characterization of Mo/Si multilayer structures by high-resolution electron microscopy. In: High Resolution Microscopy of Materials. Krakow, W., Ponce, F.A., and Smith, D.J., eds. (Mat. Res. Soc. Proc., vol. 139) pp. 339-344.

Chang, P.-H., Coviello, M.D., and Scott, A.F. (1988) Cross-sectional TEM sample preparation for multilayer electronic materials. In: Specimen Preparation for TEM of Materials. Bravman, J.C., Anderson, R.M., and McDonald, M.L., eds. (Mat. Res. Soc. Proc., vol. 115) pp. 93-97.

Garulli, A., Armigliato, A., and Vanzi, M. (1985) Preparation of cross-sections of silicon specimens for transmission electron microscopy. J. Microsc. Spectrosc. Electron., vol. 10, 2:135-145.

Gronsky, R., and Punglia, J. (1987) High-resolution electron microscopy study of a Si-Mo x-ray mirror. In: Proceedings of the 45th Annual Meeting of the Electron Microsc. Soc. of America. Bailey, G.W., ed., pp. 400-401.

Helmersson, U., and Sungren, J.-E. (1986) Cross-section preparation for TEM of film-substrate combinations with a large difference in sputtering yields. J. Electron Microsc. Tech., 4:361-369.

Holloway, K., Do, K.B., and Sinclair, R. (1988) In-situ and high-resolution TEM observation of interfacial reactions in metal-silicon multilayers. In: Multilayer: Synthesis, Properties and Non-Electronic Applications. Barbee, T.W., Spaepen, F., and Greer, L., eds. (Mat. Res. Soc. Proc., vol. 103) pp. 167-172.

Holloway, K., and Sinclair, R. (1987) Interfacial reactions in titanium-sicilon multilayers. In: Interfaces, Superlattices, and Thin Films. Dow, J.D., and Schuller, I.K., eds. (Mat. Res. Soc. Proc., vol. 77) pp. 357-362.

Kim, M.J., and Carpenter, R.W. (1987) TEM specimen heating during ion beam thinning: Microstructural stability. Ultramicroscopy, 21:327-334.

Kortright, J.B., and Denlinger, J.D. (1988) Tungsten-carbon multilayer system studied with x-ray scattering. In: Multilayers: Synthesis, Properties and Non-Electronic Applications. Barbee, T.W., Jr., Spaepen, F., and Greer, L., eds. (Mat. Res. Soc. Proc., vol. 103) pp. 95-100.

Lamble, G.M., Heald, S.M., Sayers, D.E., and Ziegler, E. (1988) Glancing angle EXAFS studies of tungsten-carbon multilayers. In Multilayers: Synthesis, Properties and Non-Electronic Applications. Barbee, T.W., Jr., Spaepen, F., and Greer, L., eds. (Mat. Res. Soc. Proc., vol. 103) pp. 101-106.

Lepetre, Y., Schuller, I.K., Rasigni, G, Rivoira, R., Phillip, R., and Dhez, P. (1985) Novel characterization of thin film multilayered structures: microleavage transmission electron microscopy. In: Applications of Thin-Film Multilayered Structures to Figured X-Ray Optics. Marshall, ed. (Proc. SPIE 563) pp. 258-264.

Lepetre, Y., Ziegler, E., Schuller, I.K., and Rivoira, R. (1986) Anomalous expansion of tungsten-carbon multilayers used in x-ray optics. J. Appl. Phys. 60, 7:2301-2303.

Marshall, G.F. (1985), editor, Applications of Thin-Film Multilayer Structures to Figured X-ray Optics. (Proc. SPIE 563, Bellingham, WA 1985).

Nguyen, T.D. (1990) Microstructural and Phase Stability Studies of Nanometer Period Metal/Carbon Multilayer Structures for X-Ray Optics. M.S. Thesis, University of California, Berkeley.

Nguyen, T.D., Gronsky, R., and Kortright, J. B. (1989) High resolution electron microscopy study of as-deposited and annealed tungsten-carbon multilayers. In: High Resolution Microscopy of Materials. Krakow, W., Ponce, F.A., and Smith, D.J., eds. (Mat. Res. Soc. Proc., vol. 139) pp. 357-362.

Nguyen, T.D., Gronsky, R., and Kortright, J.B. (1990a) Microstructure and phase stability comparison of nanometer period W/C, WC/C, and Ru/C multilayer structures. In: Thin Film Structures and Phase Stability. Clemens, B.M., and Johnson, W.L., eds. (Mat. Res. Soc. Proc.,vol. 187).

Nguyen, T.D., Gronsky, R., and Kortright, J.B. (1990b) Fresnel fringe effects at interfaces of thin multilayer structures. In: Proceedings of the Twelve International Congress for Electron Microscopy.

Nguyen, T.D., O'Keefe, M.A., Killas, R., Gronsky, R., and Kortright, J.B. (1990c) In preparation.

Petford-Long, A.K., Stearns, M.B., Chang, C.-H., Nutt, S.R., Stearns, D.G., Ceglio, N.M., and Hawryluk, A.M. (1987) High-resolution electron microscopy study of x-ray multilayer structures. J. Appl. Phys. 61, 4:1422-1428.

Ruterana, P., Chevalier, J.-P., and Houdy, P. (1989) The structure of ultrathin C/W and Si/W multilayers for high performance in soft x-ray optics. J. Appl. Phys. 65, 10:3907-3913.

Santella, M.L., Fisher, A.T., and Haltom, C.T. (1988) technique for preparing cross-section transmission electron microscopy specimens from ceramic oxide braze joints. J. Electron Microsc. Tech., 8:211-215.

Sheng, T.T., and Marcus, R.B. (1980) Advances in transmission electron microscope techniques applied to deviced failure analysis. J. Electrochem. Soc., 127:737-743.

Shih, W.C., and Stobbs, W.M. (1990) The measurement of the roughness of W/Si multilayers using the Fresnels method. Ultramicroscopy, 32:219-239.

Shinde, S.L., and De Jonghe, L.C. (1986) Cross-sectional TEM specimens from metal-ceramic composites. J. Electron Microsc. Tech., 3:361-362.

Swab, P., and Klinger, R.E. (1988) Preparation of multilayer optical coatings for TEM cross-sectional microanalysis by ultramicrotomy. In: Specimen Preparation for TEM of Materials. Bravman, J.C., Anderson, R.M., and McDonald, M.L., eds. (Mat. Res. Soc. Proc., vol. 115) pp. 229-234.

Takagi, Y., Flessa, S.A., Hart, K.L., Pawlik, D.A., Kadin, A.M., Wood, J.L., Keem, J.E., and Tyler, J.E. (1985) In: Applications of Thin-Film Multilayer Structures to Figured X-ray Optics. (Proc. SPIE 563) Marshall, G.F., ed., p. 66.

Vanhellemont, T., Bender, H., Claeys, C., van Landuyt, T., Declerck, G., Amerlinckx, S., and van Overstrateten, R. (1983) A novel sample preparation technique for cross-sectional TEM investigation of integrated circuits. Ultramicroscopy, 11:303-306.

Vanhellemont, T., Bender, H., and Rossou, L. (1988) A rapid specimen preparation technique for cross-section TEM investigation of semiconductors and metals. In: Specimen Preparation for TEM of Materials. Bravman, J.C., Anderson, R.M., and McDonald, M.L., eds. (Mat. Res. Soc. Proc., vol. 115) pp. 247-252.

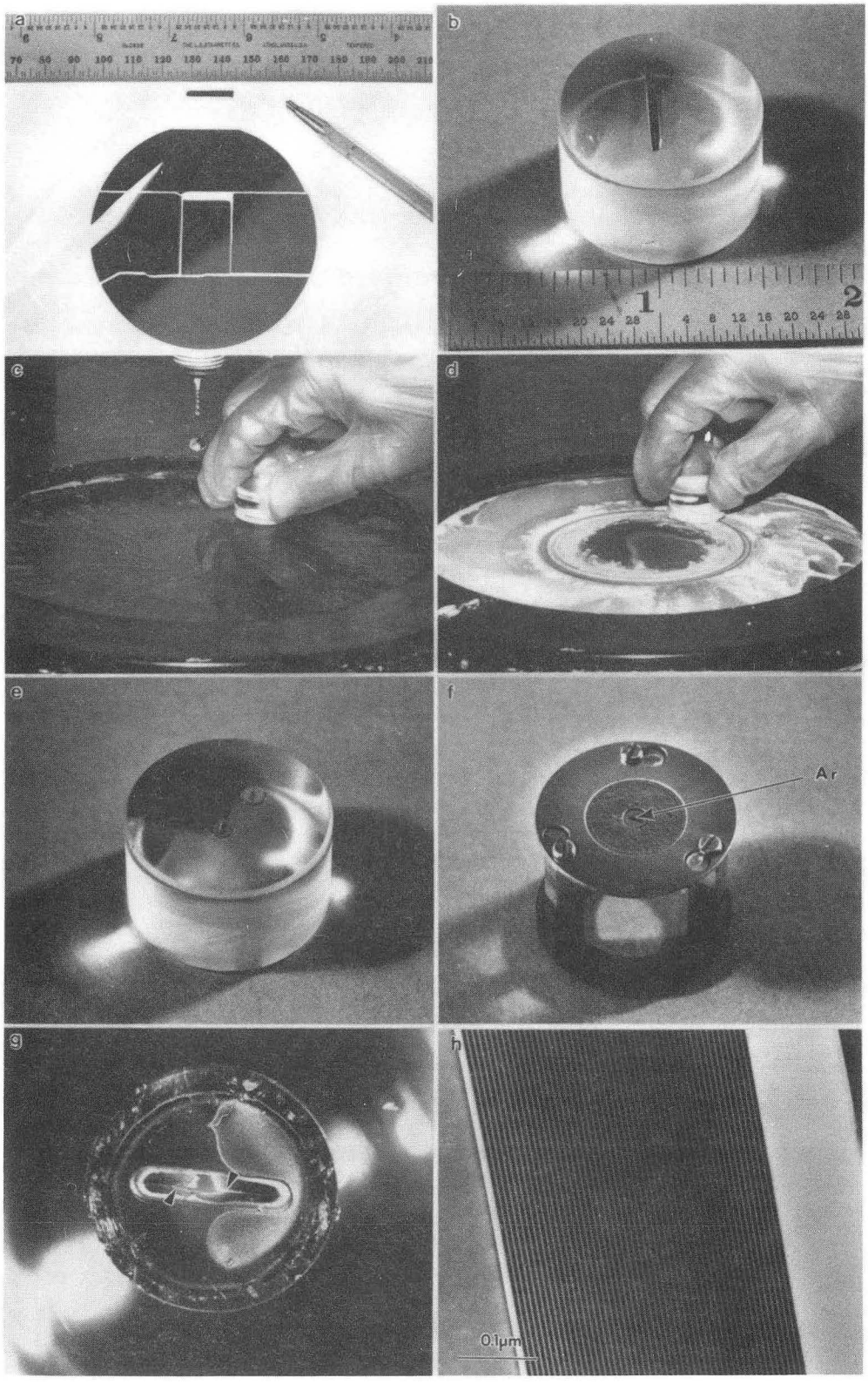

XBB 890-10823B

Figure 1 (caption next page)

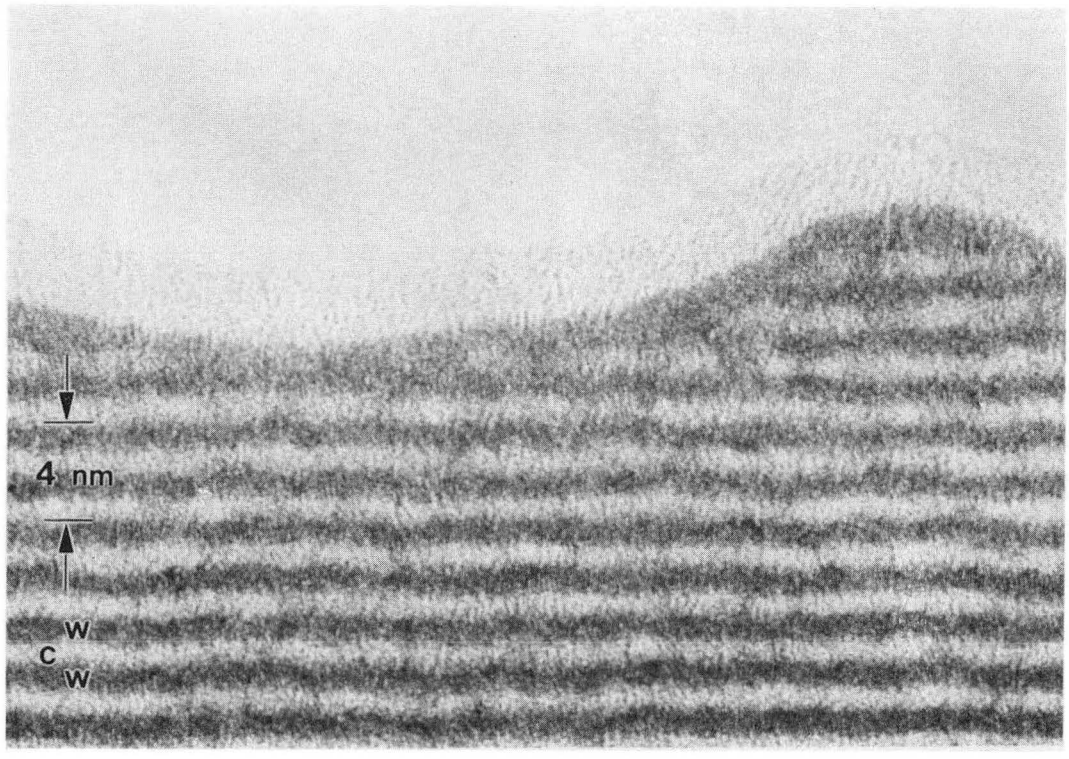

XBB 902-889

Figure 2. HRTEM micrograph of a 2 nm period W/C multilayer, showing the 3 nm amorphous thin covering layer at the edge of the sample.

Figure 1. (previous page) A procedure for preparation of cross-sectional TEM specimen:
a) two 10 mm x 3 mm slabs are cut, with the longer sides parallel to the flat edge of the Si wafer,
b) the two slab sandwich-like sample mounted on a glass support,
c) the sample is mechanically thinned on a rotating grinding wheel, and
d) polished using Alumina polishing powders,
e) after thinning, the TEM grids are mounted on the approximately 20 μm thin sample,
f) the sample is ion milled in a cold stage ion milling machine,
g) a finished sample, ready to be observed under the electron beam, with the possible observation areas arrowed,
h) a cross-sectional TEM image of a multilayer prepared by this method.

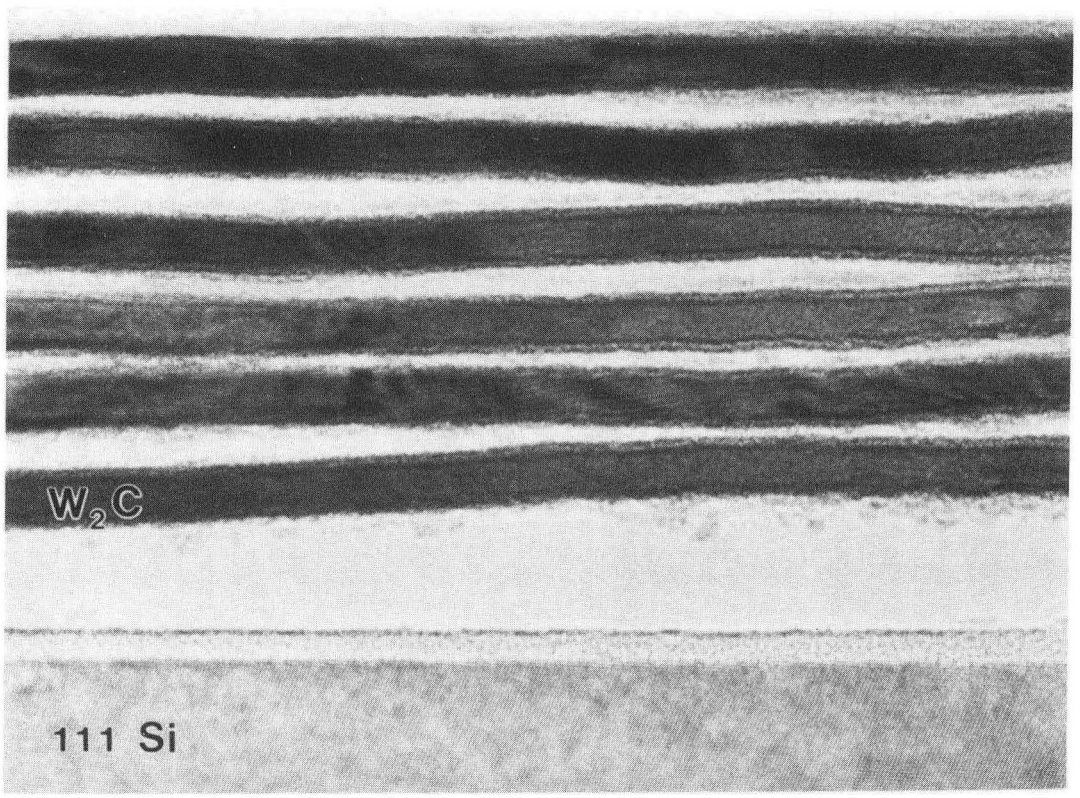

XBB 902-891

Figure 3. Example of preferential elemental ion milling. The carbon layers have been ion milled away, causing the collapsing of the tungsten layers.

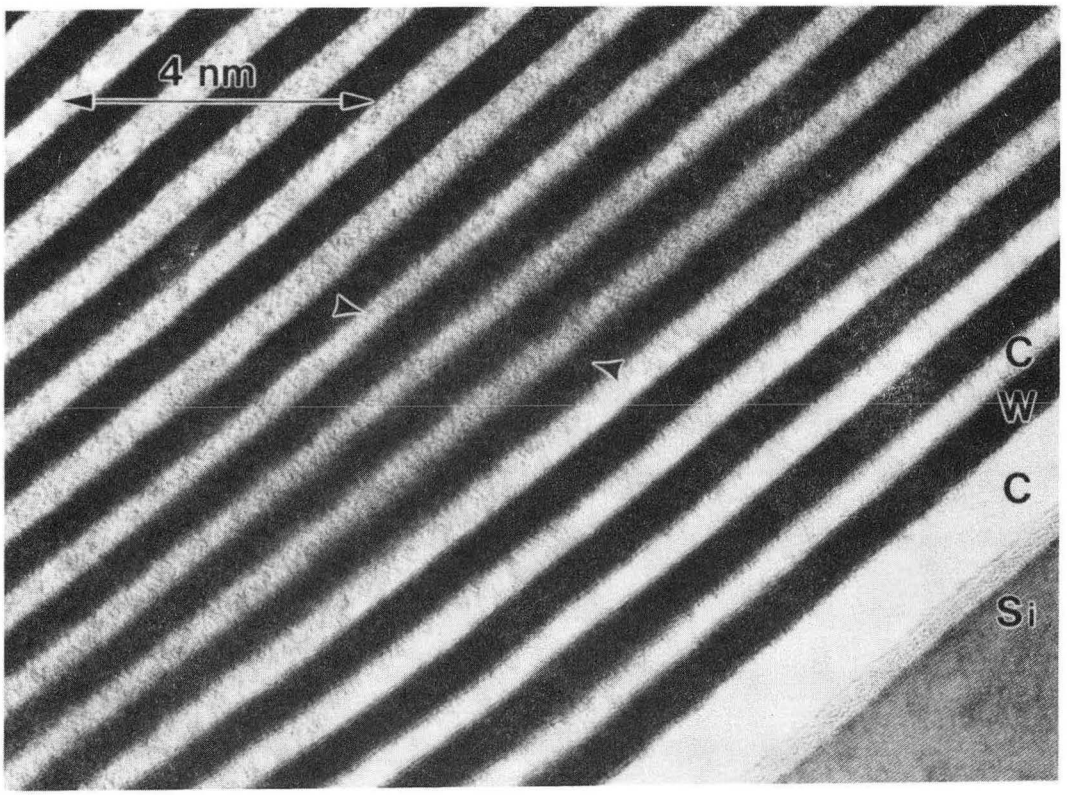

XBB 902-890

Figure 4. An "unrepresentative" area of a 7 nm period W/C multilayer. The area in arrows shows the layers, and interfaces that show different structures from the surrounding areas.

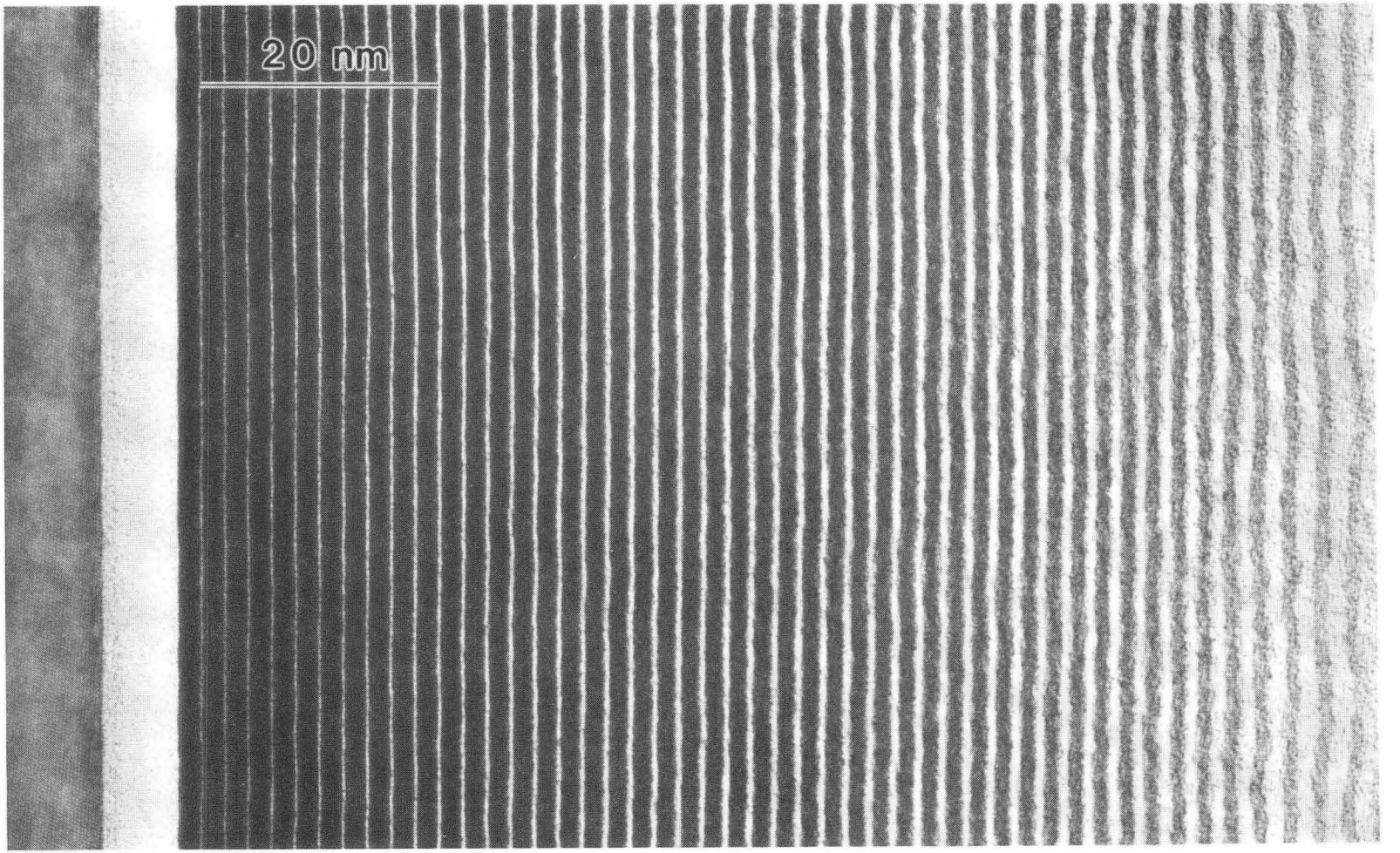

XBB 902-892

Figure 5. HRTEM of a 2 nm period W/C multilayer showing the apparent thickness variation of the layers due to possible bending of the sample under the electron beam.

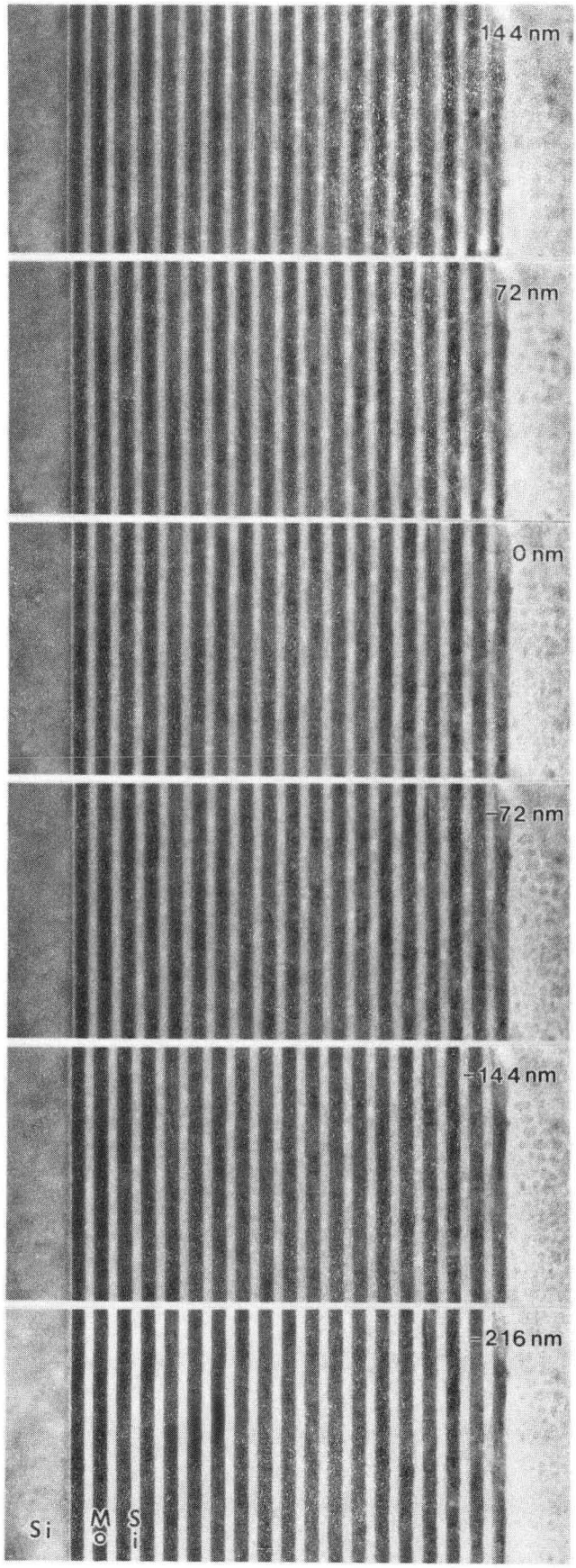

XBB 909-7956

Figure 6. A through-focus-series of a 9 nm period Mo/Si multilayer showing the effects of Fresnel fringes at interfaces. The defocus step is 72 nm.

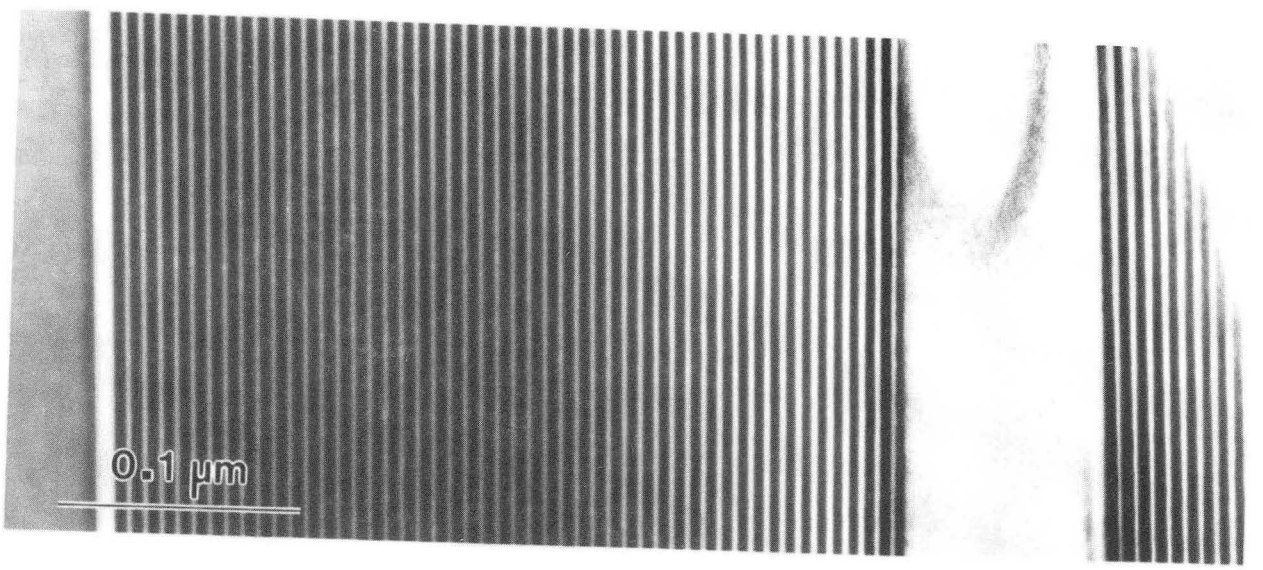

XBB 902-893

Figure 7. A low magnification electron micrograph of a full multilayer, which contains the silicon substrate, the carbon buffer layer, 50 bilayers of W and C, the epoxy layer of 80 nm thick holding the two sample slab together in the specimen preparation process, and a few bilayers of the multilayer from the other sample slab.

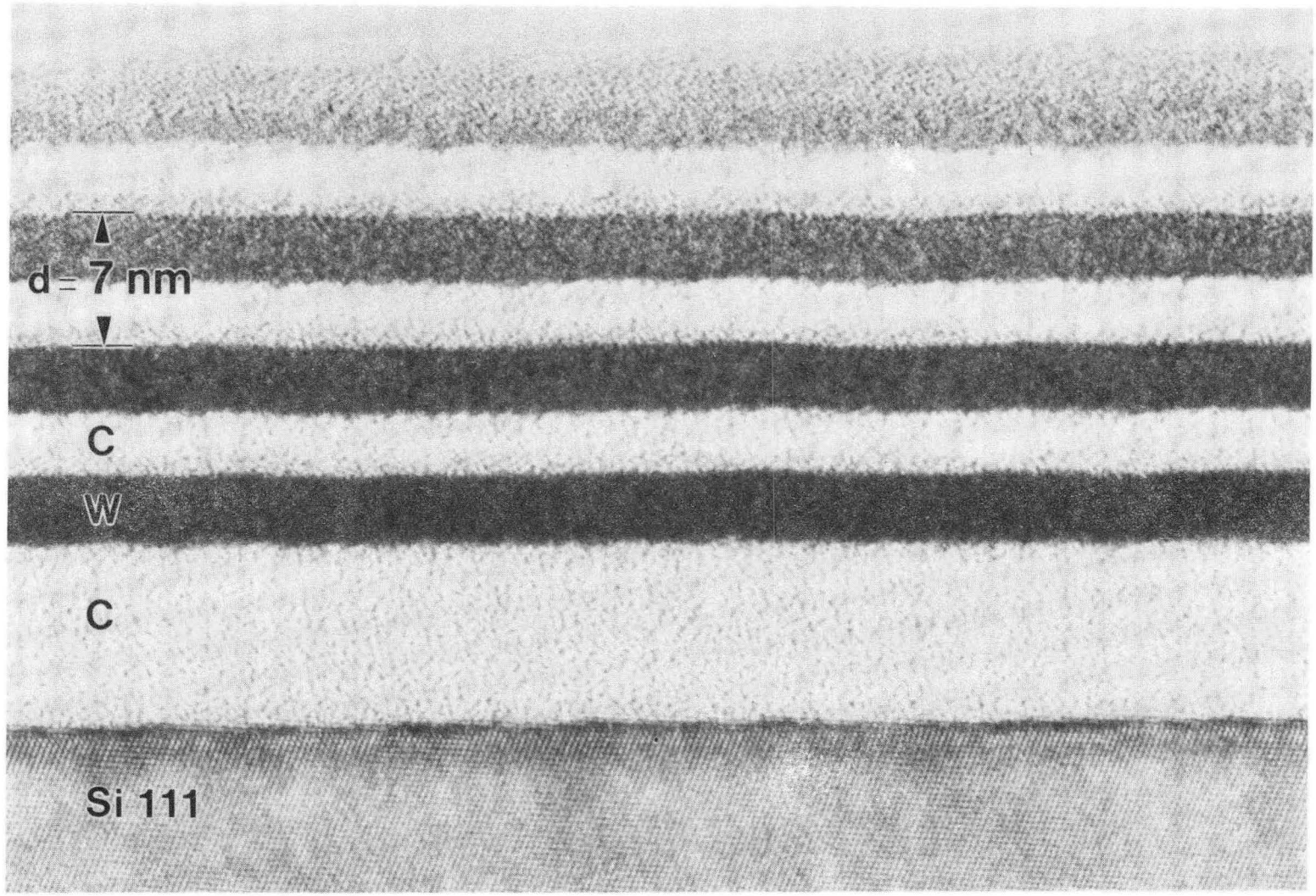

XBB 902-894

Figure 8. Closer examination of the multilayer by HRTEM technique, shown in a 7 nm period W/C multilayer.

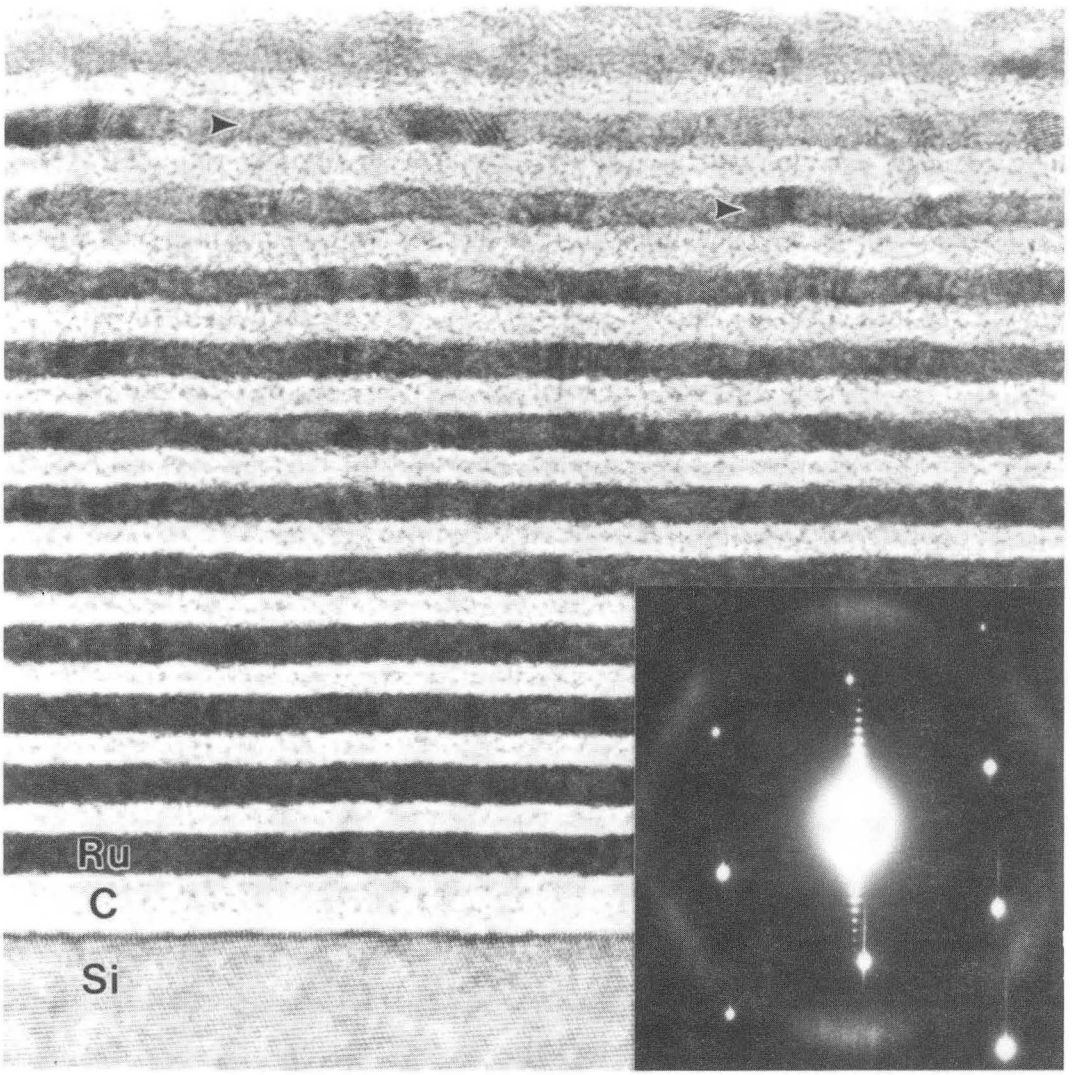

XBB 902-895

Figure 9. HRTEM of a Ru/C multilayer. The fringes in the Ru-rich layers and diffraction pattern indicate signs of crystallinity in these layers. The multilayer spots are 4.5° from exact (111) epitaxy of the substrate.

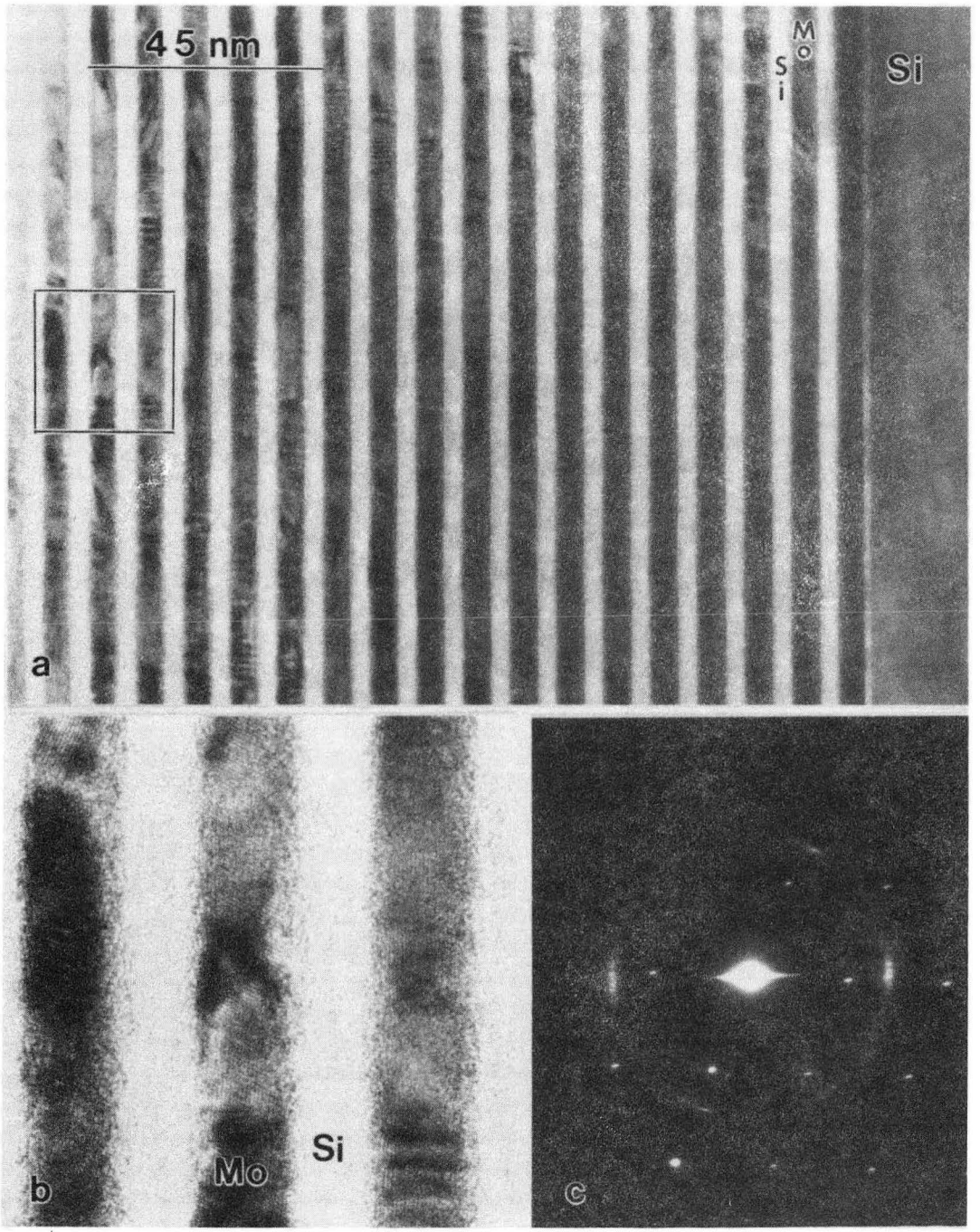

XBB 902-896

Figure 10. (a) High Resolution electron micrograph of a 9 nm period Mo/Si multilayer, (b) an enlarged image of the area indicated in (a), showing the crystalline fringes in the Mo-rich layers, and (c) the corresponding electron diffraction pattern of the multilayer.

LAWRENCE BERKELEY LABORATORY
UNIVERSITY OF CALIFORNIA
INFORMATION RESOURCES DEPARTMENT
BERKELEY, CALIFORNIA 94720